CMLS, Cell. Mol. Life Sci. 58 (2001) 823–834
1420-682X/01/060823-12 $ 1.50 + 0.20/0

CMLS Cellular and Molecular Life Sciences

Research Article

Purification, cloning and characterisation of odorant- and pheromone-binding proteins from pig nasal epithelium

A. Scaloni[a], S. Paolini[b], A. Brandazza[c], M. Fantacci[c], C. Bottiglieri[a], S. Marchese[c], A. Navarrini[c], C. Fini[b], L. Ferrara[a] and P. Pelosi[c,*]

[a] I.A.B.B.A.M.-Centro Internazionale Servizi di Spettrometria di Massa National Research Council, Via Argine 1085, 80100 Napoli (Italy)
[b] Dipartimento di Medicina Interna and Sezione INFM, University of Perugia, Via del Giochetto 6, 06126 Perugia (Italy)
[c] Dipartimento di Chimica e Biotecnologie Agrarie, University of Pisa, Via S. Michele 4, 56124 Pisa (Italy), Fax: +39 050 574235, e-mail: ppelosi@agr.unipi.it

Received 26 January 2001; received after revision 16 March 2001; accepted 19 March 2001

Abstract. Two distinct classes of lipocalin isoforms (OBP-IIs and OBP-IIIs) were purified and identified from porcine nasal mucosa of male and female individuals. Using primers designed on their N-terminal sequence, the complete primary structures of the mature polypeptides were determined. Mass spectrometry analysis confirmed the identity of the cDNA-derived sequences and provided information regarding their post-translational modifications. These species strongly resemble a lipocalin expressed by von Ebner's gland and salivary lipocalins carrying sex-specific pheromones secreted only by the boar's submaxillary glands. Both OBP-IIs and OBP-IIIs present two cysteines paired in a disulphide bond; the remaining residues occur in a reduced form. In addition, OBP-IIIs are heavily glycosylated and markedly different in their glycan moiety from the salivary lipocalins. A three-dimensional model is proposed based on protein species with known structure. Like salivary lipocalins, OBP-IIIs bind a number of odorant molecules, with highest affinity for the specific pheromone 5α-androst-16-en-3-one. The high similarity between OBPs from the nasal area and lipocalins from secretory glands suggests a common function in binding the same pheromonal ligands, the latter carrying chemical messages into the environment the former delivering them to specific receptors.

Key words. Odorant-binding protein; pig; nasal mucosa; olfaction; pheromone.

Introduction

Odorant-binding proteins (OBPs) are small soluble proteins mediating olfactory perception in vertebrates [1–5] and insects [6–9]. The physiological role played by these proteins in olfactory transduction is still largely unknown, despite the detailed structural information currently available. The complete amino acid sequence is known for a number of vertebrate OBPs, including those from frog [10], cattle [11], rat [12, 13], mouse [14, 15] and pig [16], and the three-dimensional structure has been resolved for two [17–19]. Both primary structure and crystallographic analyses clearly assign these proteins to the superfamily of 'lipocalins', soluble macromolecules generally acting as carriers of hydrophobic ligands in aqueous biological fluids [20, 21].

Their affinity and specificity for odorant molecules have been widely investigated in ligand binding assays

* Corresponding author.

[22–26]. Most of the studies have been performed with the bovine and porcine proteins, which did not reveal any major differences in binding properties. However, when two OBPs expressed in the same species are compared, as in the case of rat OBP-I and OBP-II, they demonstrate different specificities versus several odorant molecules [26]. The ligands for OBP-I share a rather flat structure, including several aromatic compounds of medium size; in contrast, those for OBP-II belong to the class of long-chain fatty acids and related compounds. The presence of a certain binding specificity, together with the microheterogeneity of these proteins reported in several animal species, could support a function for OBPs in the recognition and discrimination of different odour classes in the periphery. For this reason, we are interested in the structural and functional characterisation of distinct OBPs occurring in the same species.

We isolated and characterised the first OBP from pig, called OBP-I, which is highly expressed in the nasal respiratory region [16, 27]. Both its amino acid sequence and its binding specificity for several classes of odorants indicate close similarity to bovine OBP, to rat OBP-I, and to other macromolecules of the same sub-class. Crystallographic analysis revealed structural elements very similar to those reported for bovine OBP, although the latter occurs as a homodimer whilst pig OBP-I is a monomer [19].

Lipocalins very similar to OBPs are also found at high concentration in biological fluids known to be pheromone carriers. Mouse and rat urine contain major urinary proteins (MUP and α2-u) at concentrations of several milligrams per millilitre [28, 29]. These proteins carry pheromone molecules as endogenous ligands [30, 31]. Similar proteins are also present in the saliva of mouse [32,33] and boar [34, 35]. In the latter species, salivary lipocalins (SALs) have been shown to contain steroidal pheromone molecules as endogenous ligands. Other lipocalins involved in chemical communication are hamster aphrodisin, isolated from vaginal discharge [36–38] and apolipoprotein-D that binds the odorant heptenoic acid in human axillary sweat [39, 40].

The high similarity between OBPs from the nasal area and the lipocalins from several glands is certainly related to their affinity for the same pheromonal ligands, released into the environment through various secretions to be captured by the nasal mucus and detected. Here, we describe the purification, identification, cloning, ligand binding and structural characterisation of two additional OBPs from the pig nose, which turn out to be very similar to other proteins occurring in secretory glands, and are likely involved in chemical communication.

Materials and methods

Materials

Pig nasal mucosa from individuals of both sexes was obtained from the local abattoir. The tissue was dissected shortly after death, stored in ice and processed within 2 h. Tritiated 2-isobutyl-3-methoxypyrazine was prepared at the Amersham Laboratories (U.K.) by catalytic hydrogenation with tritium gas of the unsaturated precursor 2-(2-methyl-1-propenyl)-3-methoxypyrazine, synthesised in our laboratory (P. Pelosi, unpublished data). The pure tritiated compound had a specific activity of about 22 Ci/mmol. Mono-Q and Superose12 columns were from Pharmacia/LKB. Solvents and reagents for Edman degradation were 'sequencing' grade from Applied Biosystems, Sigma and Aldrich. All other chemicals were reagent grade.

Purification of porcine OBP-IIs and OBP-IIIs

OBP-IIs were purified from nasal tissues by anion exchange chromatography on a DE-52 column. OBP-IIIs were isolated from the same source by immunoaffinity chromatography, followed by gel filtration chromatography on a Superose12 column. For structural investigations individual components were isolated by a final chromatographic step on a Vydac C_4 column 214TP54 (250 × 4.6 mm), 5 µm, 300-Å pore size (The Separation Group). Proteins were dissolved in 0.1% trifluoroacetic acid (TFA), loaded onto the column and eluted by a linear gradient from 20% to 50% acetonitrile in 0.1% TFA over 30 min, at a flow rate of 1 ml/min.

cDNA synthesis

Total RNA was extracted from the nasal mucosa of one male and one female pig with the Trizol Reagent kit (GIBCO BRL) following the manufacturer's instructions. It was subjected to reverse transcription, using 200 units of the Moloney murine leukemia virus reverse transcriptase (GIBCO BRL) and 0.5 µg of oligo dT_{12-18} (Sigma) in 50 µl total volume. The mixture also contained 0.5 mM of each dNTP (Pharmacia Biotech, Uppsala, Sweden), 75 mM KCl, 3 mM $MgCl_2$, 10 mM dithiothreitol and 0.1 mg/ml bovine serum albumin (BSA) in 50 mM Tris-HCl, pH 8.3. The reaction mixture was incubated at 37 °C for 60 min and the products were directly used for polymerase chain reaction (PCR) amplification or stored at –20 °C.

Polymerase chain reaction

Aliquots of 1 µl crude cDNA were amplified in a Bio-Rad Gene Cycler, using 2.5 units of *Thermus aquaticus* DNA Polymerase (Sigma), 1 mM of each dNTP (Pharmacia Biotech), 1 µM of each PCR primer, 50 mM KCl, 2.5 mM $MgCl_2$ and 0.1 mg/ml BSA in 10 mM Tris-HCl, pH 8.3, containing 0.1% Triton X-100. Degenerate primers GAY-

CTNTTNGGNAGNTGGTA and AARATHGCNGGN-GARTGGTA encoding N-terminal regions of mature OBP-IIs and OBP-IIIs, respectively, were used at the 5′ end together with an oligo-dT at the 3′ end. After a denaturing step at 95 °C for 5 min , the reaction was performed for 35 cycles (95 °C for 1 min , 48 °C for 1 min , 72 °C for 1 min), followed by a final step of 7 min at 72 °C.

Cloning and sequencing

PCR products were analysed by electrophoresis on a 2% agarose gel and purified using microcolumns of the 'QIAquick PCR Purification Kit' (Qiagen). The product was then ligated into a pGEM vector (Promega) by incubating the plasmid (20 ng) and the insert in a 1:5 molar ratio overnight at room temperature. The ligation product was used to transform competent cells, prepared immediately before use. After incubation in SOC medium for 1 h at 37 °C, the cells were plated on LB/agar, containing ampicillin, isopropyl thiogalactose (IPTG) and X-Gal. White colonies were then grown in liquid LB/ampicillin and analysed for the presence of the right insert by PCR, using the plasmid primers SP6 and T7, followed by 2% agarose electrophoresis. Nucleotide sequences of both strands of the cDNA clones were determined from double-stranded plasmid DNA using the Applied Biosystem (ABI) Dye Deoxy Terminator Cycle Sequencer Kit and an ABI 310 automated sequencer at the ENEA laboratory (Casaccia, Roma, Italy).

Chemical and enzymatic reactions and peptide separation

Before carrying out sequence or mass spectrometry analysis, OBPs were alkylated under the conditions described previously [41]. Proteins were freed from excess reagents by an high-performance liquid chromatography (HPLC) purification step as described above. Carboxyamidomethylated proteins were digested with trypsin or endoprotease GluC (Boehringer Mannheim) in 0.4% ammonium bicarbonate, pH 8, at 37 °C for 16 h, using an enzyme: substrate ratio of 1:50 (w:w). Peptide mixtures were deglycosylated by 0.15 units of PNGase F incubation overnight in 0.4% ammonium bicarbonate, pH 8, at 37 °C. Peptides were fractionated by reverse-phase HPLC on a Vydac C_{18} column 214TP52 (250 × 2.1 mm), 5 µm, 300-Å pore size (The Separation Group) by using a linear gradient from 5% to 50% acetonitrile in 0.1% TFA over 60 min, at a flow rate of 0.2 ml/min. Individual components were manually collected and dried down in a Speed-vac centrifuge (Savant).

Mass spectrometry and amino acid sequence analysis

Intact proteins were submitted to electrospray mass spectrometry (ESMS) analysis using a Platform single-quadrupole mass spectrometer (Micromass). Samples were dissolved in 1% (v/v) acetic acid and 2–10 µl were injected into the mass spectrometer at a flow rate of 10 µl/min. The quadrupole was scanned from m/z 500 to 1800 at 10 s/scan and the spectra were acquired and elaborated using the MASSLYNX software. Calibration was performed by the multiply charged ions from a separate injection of myoglobin (molecular weight 16,951.5 Da). All mass values are reported as average masses.

Matrix-assisted laser desorption ionisation (MALDI) mass spectra were recorded using a Voyager DE MALDI-TOF mass spectrometer (Perkin Elmer-Perseptive Biosystem); a mixture of analyte solution, α-cyano-4-hydroxycinnamic acid and bovine insulin was applied to the sample plate and dried in vacuo. Mass calibration was performed using the molecular ions from the bovine insulin at 5734.54 Da and the matrix at 379.06 Da as internal standards. Raw data were analysed using computer software provided by the manufacturer and are reported as average masses. Assignments of the recorded mass values to individual peptides were performed on the basis of their molecular mass.

Amino acid sequences were determined using either a Perkin Elmer-Applied Biosystems 477A pulsed-liquid protein sequencer equipped with a Perkin Elmer-Applied Biosystems 120A HPLC apparatus for phenylthiohydantoin-amino acid identification, or a Milligen 6600 protein sequencer.

Endogenous ligand analysis and ligand-binding assays

Small ligands associated with the OBP-IIIs and SALs were extracted from identical amounts of protein species at room temperature with dichloromethane; the solutions were evaporated and analysed by gas chromatography-mass spectrometry (GCMS) analysis as previously reported [34]. Binding properties were measured with tritiated 2-isobutyl-3-methoxypyrazine using the filtration assay previously reported [42], or with the fluorescent ligand 1-AMA in a competitive assay [16, 27, 35].

Molecular modelling

Sequence analysis was performed using the BLASTP2 algorithm in the EXNRL-3D database. Pairwise alignments were obtained by the ClustralW multiple-alignment program [42].

Computer modelling was performed on a Silicon Graphics O2 workstation. Three-dimensional models of OBP-II isoforms were constructed on the basis of the crystallographic structure of bovine β-lactoglobulin (PDB code 1BSO), major horse allergen equC (PDB code 1EW3) and mouse major urinary protein (PDB code 1MUP); models of OBP-III isoforms were constructed on the basis of the structures of mouse major urinary protein (PDB code 1MUP), pig OBP-I (PDB code 1A3Y) and bovine OBP (PDB code 1OBP), taken from the Protein Data Bank, Brookhaven National Laboratory (Upton,

N.Y.), and using the sequence alignment obtained as described above. The N-terminal hexapeptide and C-terminal octapeptide of OBP-IIIs were not included in model construction because these residues are absent from the other sequences. All three-dimensional models were constructed with the Insight/Homology program package (Biosym). Several cycles of constrained energy minimisation regularised the structures and geometrical parameters. Models were validated using the WHATCHECK program [43].

Results

Purification and identification of porcine OBP-IIs and OBP-IIIs

Anion-exchange chromatography fractionation of a crude extract from the nasal mucosa of single pig individuals of both sexes revealed the presence of a protein with an apparent molecular weight of 17 kDa (fig. 1A), following electrophoretic analysis in denaturing conditions (SDS-PAGE). Ligand binding experiments with tritiated 2-isobutyl-3-methoxypyrazine, performed on relative chromatographic fractions, revealed an apparent binding associated with this species (data not shown). This protein was further purified and subjected to N-terminal sequencing; under these conditions, the polypeptide proved refractive to Edman degradation, indicating the presence of covalent modification at the N terminus. Sequence information was obtained after incubation with trypsin, SDS-PAGE separation of the resulting digest and Edman degradation of a selected polypeptide fragment. The sequence obtained (LVGRDPENNPEALEEF) perfectly matched that occurring in the VEG protein (residues 115–130 of the mature protein), previously isolated from pig circumvallate papillae and lachrymal glands [44]. Further evidences for the similarity between the two protein species was provided by the strong reaction of the purified OBP-IIs with antiserum against the VEG protein, as observed by Western blot experiments (fig. 1A).

Similarly, when a crude extract of nasal mucosa dissected from individuals of both sexes was analysed in Western blot experiments, strong reactivity with the antiserum against the SALs [34] was associated with an electrophoretic band of about 29 kDa (fig. 1B). In contrast sex-specific expression of SALs in only the boar's submaxillary glands has been previously reported. The protein was further purified by immunoaffinity and gel filtration chromatography, to yield a molecular species migrating as a single broad band in SDS-PAGE. As reported in the figure, it showed a higher apparent molecular mass than porcine SAL although it yielded an N-terminal sequence (HKEAGQDVVTSNFDASKIA) identical to that expected for this species.

Determination of the apparent molecular weight for OBP-IIs and OBP-IIIs by gel filtration chromatography clearly indicated the occurrence of these molecular species as monomers (data not shown).

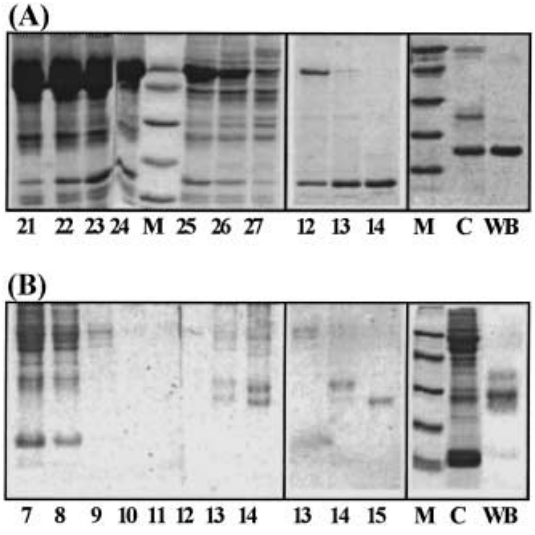

Figure 1. Purification of OBP-IIs (A) and OBP-IIIs (B) from pig nasal mucosa. Identical results were obtained for male and female individuals. (*A*) Relevant fractions obtained after DE-52 fractionation of a crude extract (lanes 21–27), purification by gel filtration on Superose12 (lanes 12–14) and the cross-reactivity of OBP-IIs with polyclonal antiserum against the pig VEG protein C, Coomassie; WB, Western blot). (*B*) Purification of OBP-IIIs by immunoaffinity chromatography, using polyclonal antibodies against the pig SALs (fractions 7–14), followed by gel filtration (fractions 13–15) and the Western blot performed on a crude extract of nasal mucosa. Molecular markers were serum albumin (66 kDa), ovalbumin (45 kDa), carbonic anhydrase (29 kDa), trypsin inhibitor (20 kDa) and α-lactalbumin (14 kDa).

Cloning and cDNA sequencing of OBP-IIs and OBP-IIIs

Based on N-terminal sequences, degenerate primers were designed, synthesised and used in PCR experiments, together with an oligo-dT, to amplify specific regions of cDNA prepared from nasal tissue RNA of single individuals of both sexes. Bands of appropriate sizes were purified and cloned into a pGEM vector, in turn used to transform competent *Escherichia coli* cells. Plasmids from positive clones were finally sequenced using plasmid primers.

Two distinct nucleotide sequences encoding OBP-II and two nucleotide sequences encoding OBP-III were detected in both individuals. The derived amino acid sequences were almost identical to those reported for porcine VEG and SAL proteins, respectively. Differences among protein isoforms were limited to a few bases and corresponded to specific amino acid substitutions (Pro141 → Leu in OBP-IIs; Val45 → Ala, Ile48 → Val and Ala73 → Val in OBP-IIIs). These data are in good agreement with the previous detection in rat of two distinct genes encoding non-allelic VEG, which probably arose by gene duplica-

tion [45]. Similar observations have also been reported for porcine SALs [35]. These genes should determine the simultaneous expression of different protein isoforms in the same pig individual.

Structural characterisation of OBP-IIs

Porcine OBP-II yielded a single chromatographic peak when analysed by reverse-phase HPLC (data not shown). As expected on the basis of the cloning results reported above, ESMS analysis of this fraction showed the presence of two different components differing by 16 Da (fig. 2). However, the measured masses did not correspond to the theoretical values calculated on the basis of the determined nucleotide sequences. Furthermore, titration with iodoacetamide under denaturing conditions resulted in a molecular mass increase of 57 Da for both species (data not shown), demonstrating that two of the three cysteine residues present in the sequence are involved in a disulphide bridge.

To verify the primary structure and ascertain the occurrence of other post-translational modifications, a reduced and carboxamidomethylated sample of protein was analysed by mass spectrometry following enzymatic digestion. An OBP-II tryptic peptide mixture was submitted directly to MALDIMS analysis; the results obtained are shown in table 1. Most of the signals recorded in the spectrum were associated with the corresponding peptide along the amino acid sequence on the basis of its mass value and trypsin specificity. The signals at m/z 2126.2 and 2142.3 were assigned to peptide (138–157) carboxamidomethyl (CAM) and its analogue bearing the amino acid replacement Pro141 → Leu, as also confirmed by amino acid sequencing. Only an unexpected mass signal at m/z 1750.9, which was unmatched with any of the calculated values for tryptic peptides, was present in the spectrum; instead, the signal at m/z 1767.9, corresponding to the peptide (1–16), was missing. The corresponding species, purified by reverse-phase HPLC, was insensitive to automated Edman degradation, suggesting the occurrence of a modified N terminus. Treatment with pyroglutamate aminopeptidase yielded a component presenting an MH^+ at m/z 1639.4, corresponding to peptide (2–16) as also revealed by amino acid sequencing, thus demonstrating the occurrence of 5-oxoproline as the N-terminal amino acid.

A parallel MALDI-mapping experiment on OBP-IIs alkylated without previous treatment with dithiothreitol allowed the nature of the cysteine residues paired in the disulphide bridge to be identified. In fact, tryptic digest revealed the occurrence of components with MH^+ at m/z 4971.9, 4955.7, 2326.9 and 2096.8 that were associated with peptides (43–69) + (138–157)Pro141 → Leu, (43–69) + (138–157), (93–111)CAM and (95–111) CAM, respectively (data not shown). These results definitively demonstrated the occurrence in porcine OBP-IIs of the disulphide Cys61-Cys152, whilst Cys101 is present in reduced form. On this basis, the mass values reported for intact OBP-IIs (fig. 3) were in perfect agreement with the theoretical values calculated for the two isoforms taking into account the presence of a disulphide bridge and a cyclized pyroglutamate residue at the N terminus (isoform A, 17,425.9 Da; isoform B, 17,441.9 Da).

Table 1. MALDIMS analysis of reduced and carboxamidomethylated OBP-IIs following digestion with trypsin.

MH^+	Peptide	Note
1750.9	(1–16)	pE1
609.5	(17–20)	
2350.9	(21–42)	
2947.4	(43–69)	CAM
1774.4	(70–84)	
918.7	(85–92)	
3223.2	(85–111)	CAM
2323.6	(93–111)	CAM
2096.5	(95–111)	CAM
1957.1	(115–131)	
2412.8	(115–135)	
1531.6	(119–131)	
2126.2	(138–157)	CAM
2142.3	(138–157)	P141L CAM

CAM, carboxamidomethyl.

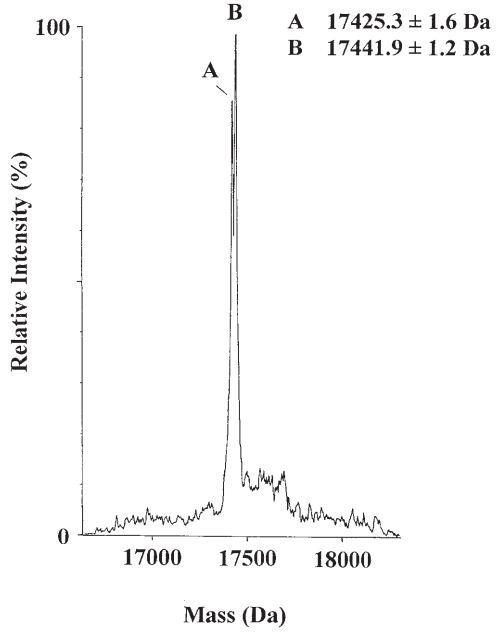

Figure 2. Transformed ESMS spectrum of OBP-II isoforms.

Structural characterisation of OBP-IIIs

The broad electrophoretic band associated with porcine OBP-IIIs and an apparent molecular weight much higher than expected on the basis of its primary structure suggested the occurrence of linked oligosaccharides, as demonstrated by concanavalin A binding after electroblotting on nitrocellulose membrane (data not shown). To

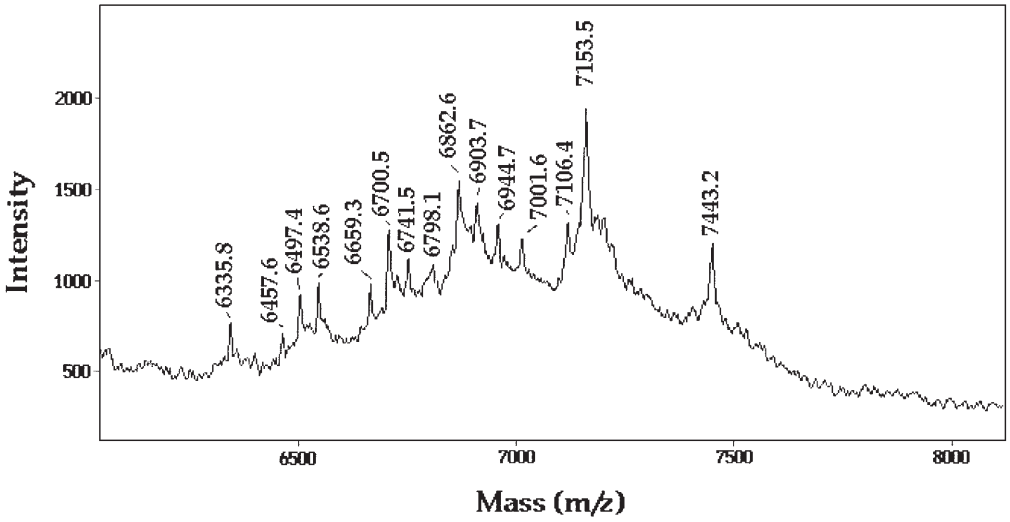

Figure 3. MALDIMS analysis of the glycopeptide components obtained from reduced and carboxamidomethylated OBP-IIIs following digestion with endoprotease GluC.

verify the occurrence of N-glycosylation phenomena already reported in the case of SAL [35], samples of OBP-IIIs were treated with N-glycosidase F. The reaction product migrated in SDS-PAGE with an apparent molecular weight lower than that of the native protein, demonstrating that OBP-III is N-glycosylated (data not shown). The same protein was refractive to the action of O-glycosidase, excluding the presence of O-glycosylation phenomena.

To verify the occurrence of distinct OBP-III isoforms, samples of reduced and carboxamidomethylated protein were analysed by mass spectrometry. A portion of the OBP-III tryptic peptide mixture obtained after PNGase F digestion was submitted directly to MALDIMS analysis. The results obtained are shown in table 2. In this case also, all the signals recorded in the spectrum were associated with the corresponding peptide along the amino acid sequence on the basis of its mass value and trypsin specificity. As expected, the spectrum showed the presence of minor MH^+ signals at m/z 857.9, 1706.7 and 1834.9, which were attributed to peptide (43–49), (64–77)CAM_2 and (63–77)CAM_2, respectively, where the amino acid replacements Val45 → Ala, Ile48 → Val and Ala73 → Val occurred. The coexistence in this mixture of the corresponding peptides not presenting these substitutions was verified by MALDIMS and amino acid sequencing following chromatographic purification. The relative intensity of the peptides measured by chromatographic and MALDIMS experiments suggested that the two isoforms were expressed at different concentrations. Complementary mass-mapping experiments carried out using endoprotease GluC as proteolytic agent confirmed these results and allowed coverage the entire protein sequence (table 2).

With the aim of identifying the N-glycosylated sites and to ascertain the nature of the polysaccharide moiety present on carboxamidomethylated OBP-IIIs, a portion of the endoprotease GluC digest before PNGase F treatment was resolved by reverse-phase HPLC and the resulting fractions were directly analysed by MALDIMS. The presence in the MALDI spectra of adjacent peaks differing

Table 2. MALDIMS analysis of tryptic and endoprotease GluC digests obtained from reduced and carboxamidomethylated OBP-IIIs following treatment with PNGase F.

Trypsin			Endoprotease GluC		
MH^+	Peptide	Note	MH^+	Peptide	Note
1833.6	(1–17)		2204.2	(1–21)	
1568.4	(3–17)		1809.4	(4–21)	
1636.7	(18–32)		1880.8	(22–37)	
1179.4	(33–42)		4068.3	(1–37)	
2798.05	(18–42)		1039.4	(38–46)	
899.7	(43–49)		1012.8	(38–46)	V45A
857.9	(43–49)	V45A, I48V	2653.8	(68–90)	2CAM
1807.2	(63–77)	2CAM	1520.4	(77–90)	
1835.5	(63–77)	A73V 2CAM	920.1	(91–97)	
1678.9	(64–77)	2CAM	2813.2	(98–121)	
1706.5	(64–77)	A73V 2CAM	2196.3	(122–139)	
1635.8	(78–92)		1252.1	(140–149)	CAM
2419.2	(95–115)		2894.1	(150–175)	CAM
1292.3	(116–125)		2520.1	(150–171)	CAM
3692.1	(95–125)		2064.8	(154–171)	CAM
812.6	(126–132)		3754.5	(140–171)	2CAM
4486.1	(95–132)		5932.1	(122–171)	2CAM
1498.4	(137–148)	CAM	4128.2	(140–175)	2CAM
945.5	(149–156)		6306.6	(122–175)	2CAM
1108.7	(157–164)	CAM			
1330.2	(149–159)				
723.3	(160–164)	CAM			
1007.8	(165–175)				

by 162, 203 and 291 mass units immediately identified the fraction containing glycopeptides. In fact, the peak eluting at 36.4 min showed the spectrum reported in figure 3. The signals observed were associated with glycosylated forms of the peptide (47–90)CAM. On the basis of the known biosynthetic pathway of N-linked oligosaccharides and the molecular mass of the peptide moiety, these signals were interpreted as the fragment (47–90)CAM bearing largely heterogeneous complex- and hybrid-type N-linked glycans on Asn53. Table 3 summarises the glycan structures identified from the MALDIMS analysis. No signal corresponding to the unglycosylated peptide was observed in the peptide mixture. On the contrary, fractions eluting at 28.6, 29.7 and 41.2 min presented intense signals at m/z 1012.4, 1039.5 and 2813.4 that were attributed to fragments (38–46) Val45 → Ala, (38–46) and (98–121), respectively. No peaks related to glycosylated forms of these peptides were observed. These findings demonstrated that Asn38 and Asn99 do not exhibit any post-translational modifications.

Parallel experiments on OBP-IIIs alkylated under denaturing conditions without treatment with reducing agents allowed us to ascertain the redox state of the cysteine residues. A combined MALDIMS-Edman degradation analysis of the tryptic digest revealed the occurrence of peptides with MH^+ at m/z 2285.7, 2413.9, 2313.8 and 2441.5 (data not shown). These components were associated with peptides (64–77)CAM + (160–164) and (63–77)CAM + (160–164) of both isoforms, where Cys68 and Cys160 were linked by a disulphide bridge and Cys75 was alkylated. These results, together with the observation that Cys141 was always contained in peptides as a carboxamidomethylated residue, demonstrated that native OBP-IIIs are characterised by the presence of the disulphide Cys68-Cys160, whilst Cys75 and Cys141 are both present in reduced form.

Table 3. MALDIMS analysis of the glycan moiety occurring in the glycopeptides resulting from endoprotease GluC digestion of carboxamidomethylated OBP-IIIs.

MH^+	Glycan composition	Structures
6335.8	$FucHexNAc_3Hex_3$	
6457.6	$FucHexNAc_2Hex_5$	
6497.4	$FucHexNAc_3Hex_4$	fucosylated monoantennary
6538.6	$FucHexNAc_4Hex_3$	
6659.3	$FucHexNAc_3Hex_5$	fucosylated diantennary hybrid
6700.5	$FucHexNAc_4Hex_4$	
6741.5	$FucHexNAc_5Hex_3$	
6798.1	$HexNAc_6Hex_3$	
6862.6	$FucHexNAc_4Hex_5$	fucosylated diantennary
6903.7	$FucHexNAc_5Hex_4$	
6944.7	$FucHexNAc_6Hex_3$	
7001.6	$HexNAc_7Hex_3$	
7106.4	$FucHexNAc_6Hex_4$	
7153.5	$SiaFucHexNAc_3Hex_5$	fucosylated monosialylated diantennary
7443.2	$Sia_2FucHexNAc_3Hex_5$	fucosylated disialylated diantennary

Fuc, fucose; HexNAc, N-acetylhexosamine, Hex, hexose.

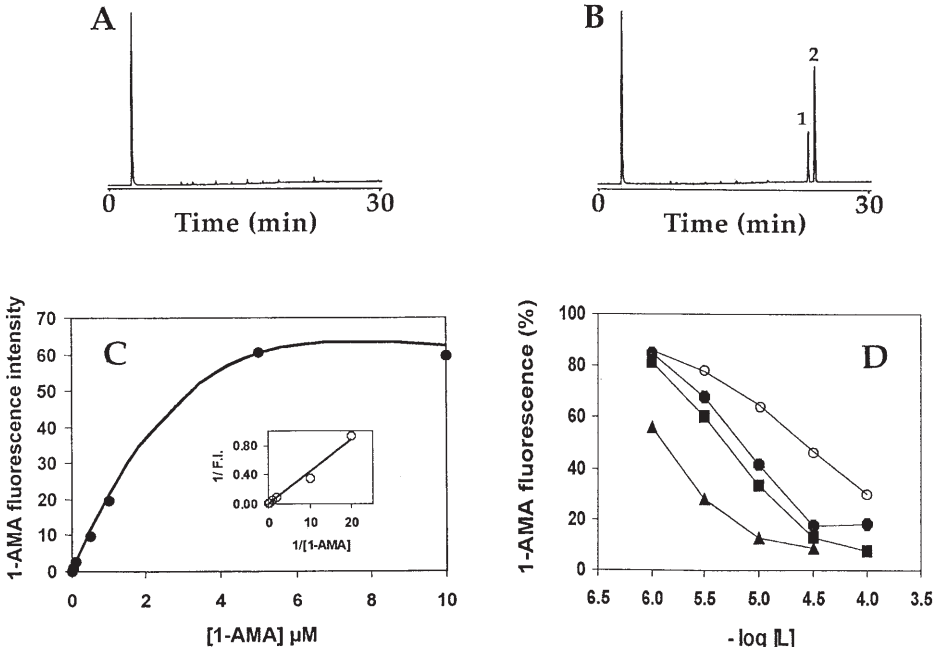

Figure 4. Comparative endogenous ligand determination by GCMS of porcine OBP-IIIs (*A*) and SALs (*B*). Peaks 1 and 2 corresponded to 5α-androst-16-en-3-ol and 5α-androst-16-en-3-one, respectively. Also shown are the ligand-binding curve (*C*) and competitive binding assays (*D*) of purified OBP-IIIs. The ligand was 1-aminoanthracene, used in fluorescence measurements as previously described [35]. The odorants employed as competitors were 5α-androst-16-en-3-one (triangles), 2-phenylethanol (closed circles), 3,7-dimethyloctanol (filled squares) and 2-isobutyl-3-methoxypyrazine (open circles).

Ligand binding experiments

Purified OBP-III and SAL samples were comparatively analysed by GCMS to ascertain the presence of endogenous ligands. Figure 4A, B reports the chromatographic profiles obtained for OBP-IIIs from female mucosa and SALs from boar submaxillary glands. Results similar to those reported in the first panel were obtained for OBP-IIIs from male individuals. These data clearly demonstrated that sex pheromones (5α-androst-16-en-3-one and 5α-androst-16-en-3-ol) are present in SALs, as previously reported [34], but are totally absent in protein samples from nasal mucosa. Similarly, the binding properties of OBP-IIIs were probed using the fluorescent ligand 1-aminoanthracene, already successfully employed with pig OBP-I [16, 27] and pig SALs [35]. The binding curve (fig. 4C) and the competitive binding measurements (fig. 4D) were similar to those measured for SALs [35]. This is hardly surprising given the structural similarities between the proteins. On the other hand, according to the similar behaviour observed for SAL in its native (glycosylated) and recombinant (non-glycosylated) forms, the larger glycan moiety observed in OBP-IIIs was not expected to be relevant for the binding properties of the species [35]. These observations suggest that sex pheromones could also be the physiological ligand for OBP-IIIs, temporarily captured by the protein following their release into the environment as chemical messages. In contrast no reliable binding data were obtained for OBP-IIs. The ligand used for most OBPs, 2-isobutyl-3-methoxypyrazine, showed only weak binding, while the fluorescent probe 1-aminoanthracene was inefficient. Tritium labelled palmitic acid also proved to be a weak ligand in a filtration assay, while fluorescence measurements using retinol as the ligand detected some binding to OBP-IIs, but a binding curve could not be determined. Other potential ligands have not been tested so far.

Molecular modelling

The sequence identity in pairwise comparisons between OBP-IIs, OBP-IIIs and members of the lipocalin family whose three-dimensional structure is known was about 40% or less. Nevertheless, on the basis of the homology observed and secondary-structure predictions, we hypothesise a lipocalin fold for both molecular species. For our modelling, we generated a secondary-structure-driven sequence alignment between porcine OBP-IIs, bovine β-lactoglobulin [46], major horse allergen equC [47] and mouse major urinary protein [48]; a similar procedure was used for porcine OBP-IIIs, mouse major urinary protein [48], porcine OBP-I [19] and bovine OBP [17, 18]. Both alignments were submitted to the same modelling procedure. Figure 5 shows the general folding pattern of OBP-II and OBP-III molecules. In both cases, models obtained using the amino acid sequence of the other isoforms described in this paper were entirely superimposable on that shown in the figure. The superimposed backbone traces of OBP-IIs with mouse major urinary protein displayed a 1.2 Å root-mean-square deviation (RMSD) on 152 Cα atoms. Good values were also obtained in the superimposition with the major horse allergen equC (1.5 Å RMSD on 152 Cα atoms) and in part with bovine β-lactoglobulin (1.9 Å RMSD on 146 Cα atoms). A good superimposition was also obtained in the case of OBP-IIIs with mouse major urinary protein (0.6 Å RMSD on 152 Cα atoms), with porcine OBP-I (1.5 Å RMSD on 142 Cα atoms) and in part with bovine OBP (1.7 Å RMSD on 105 Cα atoms). The Ramachandran plots indicated that most of the residues (95% for OBP-IIs and 96% for OBP-IIIs) present φ and ψ angles in the core and allowed regions, except for proline and glycine residues and a few amino acids located in loop regions (data not shown). Most bond lengths, bond and torsion angles were in the range of values expected for a naturally folded protein (data not shown). The schematic structural models shown consists of the typical nine-stranded β barrel containing three (OBP-IIs) or two (OBP-IIIs) helices observed in other members of the lipocalin family (fig. 5A, B). The secondary structure elements identified in OBP-IIs were α1 (Gln11-Asp12), β1 (Gly15-Asp25), α2 (Ile28-Gly30), β2 (Thr37-Leu44), β3 (Asp48-Ile57), β4 (Gln60-Leu68), β5 (Phe77-Ala79), β6 (Lys83-Leu89), β7 (Asp95-Glu104), β8 (Val110-Arg118), α3 (Pro124-Lys137) and β9 (Val144-Pro146). Similarly, these elements in OBP-IIIs were β1 (Gly20-Asp30), α1 (Lys32-Glu36), β2 (Phe44-Leu51), β3 (Ser55-Val64), β4 (Glu66-Val78), β5 (Val82-Tyr87), β6 (Gly89-Asn99), β7 (Asp102-Asn112), β8 (Lys115-Arg125), α2 (Pro131-Gln143) and β9 (Asn150-Leu154).

Both models revealed the presence of a flat hydrophobic cavity inside the β-barrel able to accommodate the polycyclic molecules observed as natural and synthetic ligands. Furthermore, the figure illustrates that in the case of OBP-IIIs, the amino acid replacements observed are all located in the hydrophobic pocket of the protein; in contrast, the single amino acid substitution occurring in OBP-IIs is placed in a loop region far from the binding cavity. Comparison of the models reported in the figure also highlighted the main structural differences between the two porcine proteins reported in this study. A careful analysis revealed the presence in OBP-IIIs of longer secondary-structural elements (β5, β6, β7 and β8) with respect to OBP-IIs that could affect relative protein stability.

Furthermore, structural analysis in the region 113–128 of OBP-IIs and 120–135 of OBP-IVs revealed Asp119 (OBP-IIs) and Lys126 (OBP-IIIs) as major elements responsible for the narrow turn present in both proteins between β8 and α3 and β8 and α2, respectively. This polypeptide segment was reported as crucial in the domain swapping observed in bovine OBP and responsible for

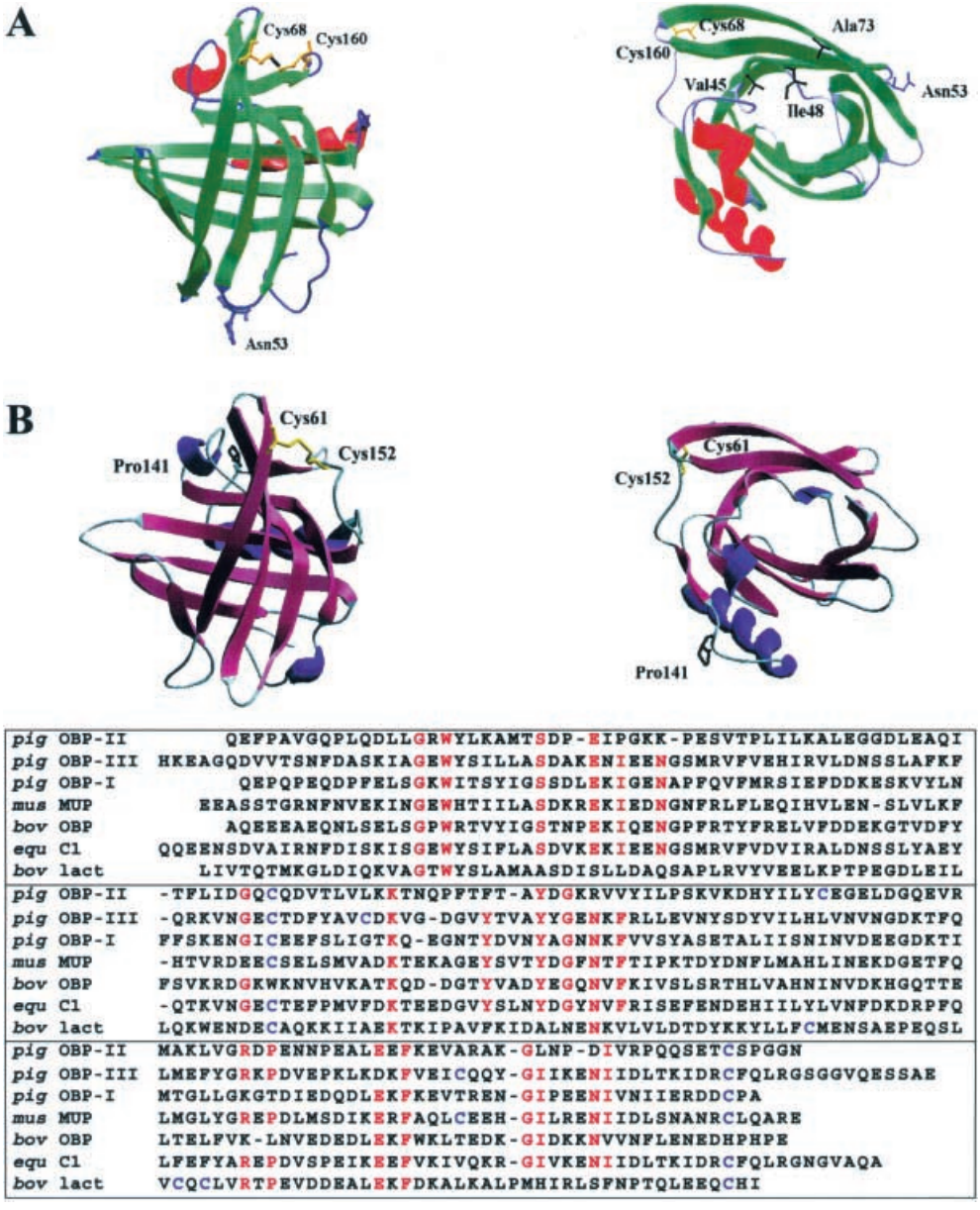

Figure 5. Two different views of the three-dimensional structure of OBP-IIIs (*A*) and OBP-IIs (*B*) models. The β sheet regions are indicated in green (OBP-IIIs) and magenta (OBP-IIs), the α helices in red (OBP-IIIs) and dark blue (OBP-IIs). In both cases, loops and disulphide bridges are highlighted in light blue and yellow, respectively. The amino acid residues involved in post-translational modifications and isoform replacements are indicated. The sequence alignment of porcine OBPs with lipocalins whose three-dimensional structure is known is also shown. Conserved amino acid residues and cysteines are highlighted in red and blue, respectively.

protein dimerisation [19]. Primary-structure alignment (fig. 5) revealed high sequence homology in this region between OBP-IIs, OBP-IIIs, mouse major urinary protein, porcine OBP-I and major horse allergen equC, whilst in bovine OBP, a deletion was observed. Therefore, the presence of a longer and more flexible segment should allow a narrower turn in the molecular structure, generating the monomeric form observed in the case of native OBP-IIs and OBP-IIIs. Furthermore, the presence in these proteins of a disulphide bridge (Cys61-Cys152 in OBP-IIs and Cys68-Cys160 in OBP-IIIs) conserved in the other lipocalins prevent any possible molecular rearrangement associated with domain swapping phenomena.

Discussion

This study reports the isolation of two distinct protein families from the pig nasal mucosa of individuals of both sexes, with structures very closely related to VEG and SAL proteins, previously reported in secretory glands of

the same species. Given their affinity for odorants and pheromones and their expression in the nasal area, these proteins have been classified as OBPs. These findings provide additional evidence that the same proteins are used in different regions of the body delivering and for capturing chemical messengers.

The role played by saliva in chemical communication is less well known and documented than is the case for urine; however, its fuction has been definitely established in at least some species, such as mouse [49] and pig [50]. The boar sex pheromones (5α-androst-16-en-3-one and 5α-androst-16-en-3-ol) were among the first mammalian pheromonal molecules to be identified and the saliva was early recognised as their carrier [51]. The SAL proteins are the major components secreted by the boar's submaxillary glands, while they are completely absent in the sow. This sex-specific expression and their ability to bind boar pheromones as endogenous ligands clearly defines the physiological function of these proteins in delivering the chemical messengers in the environment [35].

The similar amino acid sequence, oxidation state and binding properties of OBP-IIIs and SALs indicates that the nasal proteins could perform a similar function in collecting steroid pheromones from the environment and carrying them to the sensory neurones of the vomeronasal organ. Nevertheless, while the binding cavity of SALs purified from submaxillary glands contains pheromone molecules [34], its nasal counterpart (OBP-IIIs) is devoid of any ligand. Moreover, unlike SALs, OBP-IIIs are expressed in both sexes. Therefore, only males can use SALs and their endogenous ligands to mark the territory; in contrast, both males and females can detect the closeness of male individuals using OBP-IIs to perceive their sexual messengers.

A further similarity between the salivary lipocalins and the nasal OBP-IIIs is the expression in both tissues of at least two genes, whose products differ by three amino acid substitutions. All these substitutions occur inside the ligand-binding cavity. It is tempting to speculate that the two forms of OBP-III and SAL are specific for two pheromone components. Concerning the role played by the glycan part of the proteins, we cannot suggest hypotheses on the basis of the available data. Both SALs and OBP-IIIs are N-glycosylated only at Asn53, but the OBP-IIIs glycan moiety is much larger and more complex. These results could be related to the differential expression of enzymes involved in the biosynthetic pathway of the glycoproteins in the distinct tissues from which the proteins have been purified.

The identity of a physiological ligand for OBP-IIs is far from resolved. For the VEG proteins (identical to OBP-IIs), the data reported in the literature are not in full agreement. We used retinol in fluorescence assays, based on the report that this molecule was a good ligand for the human protein [52]. However, our data, although indicating the presence of a measurable binding activity, showed poor reproducibility and could not be used to build a reliable saturation curve. Therefore, while the role of SALs/OBP-IIIs as pheromone carriers is beyond doubt, the physiological function of VEGs/OBP-IIs is still uncertain. In humans and in the pig, the same protein is expressed by nasal glands and von Ebner's glands, while in the rat, the nasal protein is only 45% identical with the VEG protein. The VEG protein, moreover, is also expressed in lachrymal glands [52] (where it is named tear lipocalin), in the prostate [53] and in the pituitary glands. Its proteinase-inhibiting activity [54] as well as its affinity for retinol and fatty acids suggested that VEG proteins could perform a function in protecting mucosal tissues. However all the organs where the VEG protein has been described so far are in some way related to sexual function and chemical communication, although this might just be a coincidence and certainly no hypothesis for the role of these proteins can be based in these observations. Investigating the presence of endogenous ligands for proteins of the VEG family when secreted by different glands could certainly provide interesting information for understanding their physiological function.

Acknowledgements. This work was supported by EEC grand no. BIO4-CT98-0420 to P.P.

1 Pelosi P., Baldaccini N. E. and Pisanelli A.M. (1982) Identification of a specific olfactory receptor for 2-isobutyl-3-methoxypyrazine. Biochem. J. **201:** 245–248
2 Pelosi P. (1994) Odorant-binding proteins. Crit. Rev. Biochem. Mol. Biol. **29:** 199–228
3 Pelosi P. (1996) Perireceptor events in olfaction. J. Neurobiol. **30:** 3–19
4 Pelosi P. (1998) Odorant-binding proteins: structural aspects. Ann. NY Acad. Sci. **855:** 281–293
5 Tegoni M., Pelosi P., Vincent F., Spinelli S., Campanacci V., Grolli S. et al. (2000) Mammalian odorant binding proteins. Biochim. Biophys. Acta **1482:** 229–240
6 Vogt R.G. and Riddiford L. M. (1981) Pheromone binding and inactivation by moth antennae. Nature **293:** 161–163
7 Pelosi P. and Maida R. (1995) Odorant-binding proteins in insects. Comp. Biochem. Physiol. **111B:** 503–514
8 Vogt R. G., Rybczynski R. and Lerner M. R. (1990) The biochemistry of odorant reception and transduction. In: Chemosensory Information Processing, NATO ASI Series H, vol. 39, pp. 33–76, Schild D. (ed.), Springer, Berlin
9 Steinbrecht R. A. (1998) Odorant-binding proteins: expression and function. Ann. NY Acad. Sci. **855:** 323–332
10 Lee H. K., Wells, R. G. and Reed R. R. (1987) Isolation of an olfactory cDNA: similarity to retinol binding protein suggests a role in olfaction. Science **253:** 1053–1056
11 Tirindelli R., Keen J. N., Cavaggioni A., Eliopoulos E. E. and Findlay J. B. C. (1989) Complete aminoacid sequence of pyrazine-binding protein from cow nasal mucosa. Eur. J. Biochem. **185:** 569–572
12 Pevsner J., Hwang P. M., Sklar P. B., Venable J. C. and Snyder S. H. (1988) Odorant-binding protein and its mRNA are localised to lateral nasal gland implying a carrier function. Proc. Natl. Acad. Sci. USA **85:** 2383–2387

13 Dear T. N., Campbell K. and Rabbitts T. H. (1991) Molecular cloning of putative odorant-binding and odorant-metabolizing proteins. Biochemistry **30:** 10376–10382
14 Miyawaki A., Matsushita F., Ryo Y. and Mikoshiba K. (1994) Possible pheromone-carrier function of two lipocalin proteins in the vomeronasal organ. EMBO J. **13:** 5835–5842
15 Pes D., Mameli M., Andreini I., Krieger J., Weber M., Breer H. et al. (1998) Cloning and expression of odorant-binding proteins Ia and Ib from mouse nasal tissue. Gene **212:** 49–55
16 Paolini S., Scaloni A., Amoresano A., Marchese S., Napolitano E. and Pelosi P. (1998) Amino acid sequence, post-translational modifications, binding and labelling of porcine odorant-binding protein. Chem. Senses **23:** 689–698
17 Bianchet M. A., Bains G., Pelosi P., Pevsner J., Snyder S. H., Monaco H. L. et al. (1996) The three dimensional structure of bovine odorant-binding protein and its mechanism of odor recognition. Nat. Struct. Biol. **3:** 934–939
18 Tegoni M., Ramoni R., Bignetti E., Spinelli S. and Cambillau C. (1996) Domain swapping creates a third putative combining site in bovine odorant binding protein dimer. Nat. Struct. Biol. **3:** 863–867
19 Spinelli S., Ramoni R., Grolli S., Bonicel J., Cambillau C. and Tegoni M. (1998) The structure of the monomeric porcine odorant binding protein sheds light on the domain swapping mechanism. Biochemistry **37:** 7913–7918
20 Flower D. R. (1996) The lipocalin protein family: structure and function. Biochem. J. **318:** 1–14
21 Paine K. and Flower D.R. (2000) The lipocalin website. Biochim. Biophys. Acta **1482:** 351–352
22 Pelosi P. and Tirindelli R. (1989) Structure-activity studies and characterization of an odorant-binding protein. In: Chemical Senses: Receptor Events and Transduction in Taste and Olfaction, vol. 1, pp. 207–226, Brand J. G., Teeter J. H., Cagan R. H. and Kare M. R. (eds), Dekker, New York
23 Pevsner J., Hou V., Snowman A. M. and Snyder S. H. (1990) Odorant-binding protein, characterization of ligand binding. J. Biol. Chem. **265:** 6118–6125
24 Hérent M. F., Collin S. and Pelosi P. (1995) Affinities of nutty and green-smelling pyrazines and thiazoles to odorant-binding proteins, in relation with their lipophilicity. Chem. Senses **20:** 601–608
25 Dal Monte M., Andreini I., Revoltella R. and Pelosi P. (1991) Purification and characterization of two odorant-binding proteins from nasal tissue of rabbit and pig. Comp. Biochem. Physiol B. **99:** 445–451
26 Loebel D., Marchese S., Krieger J., Pelosi P. and Breer H. (1998) Subtypes of odorant binding proteins: heterologous expression and assessment of ligand binding. Eur. J. Biochem. **254:** 318–324
27 Paolini S., Tanfani F., Fini C., Bertoli E. and Pelosi P. (1999) Porcine odorant-binding protein: structural stability and ligand affinities measured by fourier-transform infrared spectroscopy and fluorescence spectroscopy. Biochim. Biophys. Acta **1431:** 179–188
28 Cavaggioni A., Findlay J. B. C. and Tirindelli R. (1990) Ligand binding characteristics of homologous rat and mouse urinary proteins and pyrazine binding protein of the calf. Comp. Biochem. Physiol. **96B:** 513–520
29 Robertson D. H., Cox K. A., Gaskell S. J., Evershed R. P. and Beynon R. J. (1996) Molecular heterogeneity in the major urinary proteins of the house mouse *Mus musculus*. Biochem. J. **316:** 265–272
30 Bacchini A., Gaetani E. and Cavaggioni A. (1992) Pheromone-binding proteins in the mouse *Mus musculus*. Experientia **48:** 419–421
31 Robertson D. H. L., Beynon R. J. and Evershed R. P. (1993) Extraction, characterisation and binding analysis of two pheromonally active ligands associated with major urinary protein of the house mouse (*Mus musculus*). J. Chem. Ecol. **19:** 1405–1416
32 Shahan K. M., Denaro M., Gilmartin M., Shi Y. and Derman E. (1987) Expression of six mouse major urinary protein genes in the mammary, parotid, sublingual, submaxillary and lachrymal glands and in the liver. Mol. Cell. Biol. **7:** 1947–1954
33 Shaw P. H., Held W. A. and Hastie N. D. (1983) The gene family for major urinary proteins: expression in several secretory tissues of the mouse. Cell **32:** 755–761
34 Marchese S., Pes D., Scaloni A., Carbone V. and Pelosi P. (1998). Lipocalins of boar salivary glands binding odours and pheromones. Eur. J. Biochem. **252:** 563–568
35 Loebel D., Scaloni A., Paolini S., Fini C., Ferrara L., Breer H. et al. (2000) Cloning, post-translational modifications, heterologous expression and ligand-binding of boar salivary lipocalin. Biochem J. **350:** 369–379
36 Singer A. G. and Macrides F. (1993) Composition of an aphrodisiac pheromone. Chem. Senses **18:** 630–636
37 Henzel W. J., Rodriguez H., Singer A. G., Stults J. T., Macrides F., Agosta W. C. et al. (1988) The primary structure of aphrodisin. J. Biol. Chem. **263:** 16682–16687
38 Magert H. J., Hadrys T., Cieslak A., Groger A., Feller S. and Forssmann W. G. (1995) DNA sequence and expression pattern of the putative pheromone carrier aphrodisin. Proc. Natl. Acad. Sci. USA **92:** 2091–2095
39 Spielman A., Zeng X. N., Leyden J. and Preti G. (1995) Proteinaceous precursors of human axillary odor: isolation of two novel odor-binding proteins. Experientia **51:** 40–47
40 Zeng C., Spielman A., Vowels B. R., Leyden J., Biemann K. and Preti G. (1996) A human axillary odorant is carried by apolipoprotein D. Proc. Natl. Acad. Sci. USA **93:** 6626–6630
41 Scaloni A., Monti M., Angeli S. and Pelosi P. (1999) Structural analysis and disulfide-bridge pairing of two odorant-binding proteins from *Bombyx mori*. Biochem. Biophys. Res. Commun. **266:** 386–391
42 Thompson J., Higgins G. and Gibson T. J. (1994) Clustal W: improving the sensitivity of progressing multiple sequence alignment through sequence weighting, position-specific gap penalties and weight matrix choice Nucleic Acids Res. **22:** 4673–4680
43 Hooft R. W. W., Vriend G., Sander C. and Abola E. E. (1996) Errors in protein structures. Nature **381:** 272–280
44 Garibotti M., Christiansen H., Schmale H. and Pelosi P. (1995) Porcine VEG proteins and tear prealbumins. Chem. Senses **20:** 69–76
45 Kock K., Ahlers C. and Schmale H. (1994) Structural organization of the genes for rat von Ebner's gland proteins 1 and 2 reveals their close relationship to lipocalins. Eur. J. Biochem. **221:** 905–916
46 Sawyer L. and Kontopidis G. (2000) The core lipocalin, bovine beta-lactoglobulin. Biochim. Biophys. Acta **1482:** 136–148
47 Lascombe M., Gregoire C., Poncet P., Tavares G., Rosinski-Chupin I., Rabillon J. et al. (2000) Crystal structure of the allergen Equc 1: a dimeric lipocalin with restricted IgE-reactive epitopes. J. Biol. Chem. **275:** 21572–21577
48 Böcskei Z., Groom C. R., Flower D. R., Wright C. E., Phillips E.V., Cavaggioni A. et al. (1992) Pheromone binding to two rodent urinary proteins revealed by X-ray crystallography. Nature **360:** 186–188
49 Marchlewska-Koj A., Pochron E. and Sliwowska A. (1990) Salivary glands and preputial glands of males as source of estrus-stimulating pheromone in female mice. J. Chem. Ecol. **16:** 2817–2822
50 Booth W. D. and von Glos K. I. (1991) Pheromaxein, the pheromonal steroid-binding protein, is a major protein synthesized in porcine submaxillary salivary glands. J. Endocrinol. **128:** 205–212
51 Katkov T., Booth W. D. and Gower D. B. (1972) The metabolism of 16-androstenes in boar salivary glands. Biochim. Biophys. Acta **270:** 546–556

52 Redl B., Holzfeind P. and Lottspeich F. (1992) cDNA cloning and sequencing reveals human tear prealbumin to be a member of the lipophilic-ligand carrier protein superfamily. J. Biol. Chem. **267:** 20282–20287
53 Holzfeind P., Merschak P., Rogatsch H. Culig Z., Feichtinger H., Klocker H. et al. (1996) Expression of the gene for tear lipocalin/von Ebner's gland protein in human prostate. FEBS Lett. **395:** 95–98
54 van't Hof W., Blankenvoorde M. F., Veerman E. and Amerongen A.V. (1997) The salivary lipocalin von Ebner's gland protein is a cysteine proteinase inhibitor. J. Biol. Chem. **272:** 1837–1841